International Journal for Multiscale Computational Engineering, 2(4)599-619(2004)

Computational Evaluation of Strain Gradient Elasticity Constants

R.H.J. Peerlings*

Department of Mechanical Engineering,
Eindhoven University of Technology
PO Box 513, 5600 MB Eindhoven, The Netherlands

N.A. Fleck[1]

Department of Engineering, University of Cambridge
Trumpington Street, Cambridge, CB2 1PZ, UK

ABSTRACT

Classical effective descriptions of heterogeneous materials fail to capture the influence of the spatial scale of the heterogeneity on the overall response of components. This influence may become important when the scale at which the effective continuum fields vary approaches that of the microstructure of the material and may then give rise to size effects and other deviations from the classical theory. These effects can be successfully captured by continuum theories that include a material length scale, such as strain gradient theories. However, the precise relation between the microstructure, on the one hand, and the length scale and other properties of the effective modeling, on the other, are usually unknown. A rigorous link between these two scales of observation is provided by an extension of the classical asymptotic homogenization theory, which was proposed by Smyshlyaev and Cherednichenko (J. Mech. Phys. Solids 48:1325–1358, 2000) for the scalar problem of antiplane shear. In the present contribution, this method is extended to three-dimensional linear elasticity. It requires the solution of a series of boundary value problems on the periodic cell that characterizes the microstructure. A finite element solution strategy is developed for this purpose. The resulting fields can be used to determine the effective higher-order elasticity constants required in the Toupin-Mindlin strain gradient theory. The method has been applied to a matrix-inclusion composite, showing that higher-order terms become more important as the stiffness contrast between inclusion and matrix increases.

*Corresponding author: r.h.j.peerlings@tue.nl

[1]Email: naf1@eng.cam.ac.uk

1. INTRODUCTION

Despite the fact that the deformation of solid materials is ultimately governed by the motion of atoms and the forces acting between them, engineers generally successfully rely on continuum theories that describe the effect of these phenomena at a much larger scale and in an average sense. The main motivation for using such approximate theories is efficiency; even on modern digital computers, full-scale atomistic simulations of engineering structures and components simply require too much computational power to be of practical use to a designer. Furthermore, such computations, which depend on more or less arbitrarily chosen initial conditions, would deliver far more detail than is required. Continuum theories, such as linear elasticity, plasticity, etc., provide the approximate response engineers are interested in at a fraction of the cost of even the simplest atomistic simulation.

Most materials exhibit some kind of order at one or several spatial scales between the atomic scale and that of components and structures. Examples are the crystal lattice in metals and the arrangement of fibers and matrix in fiber-reinforced laminates. Where this order is imperfect or even entirely absent, a number of spatial scales usually can still be distinguished in the disorder. For instance, grains in a metallic component tend to have a rather uniform size, even if their shape may be disordered. Likewise, these and other materials may contain voids and defects whose size and spacing have a typical order of magnitude. Standard elasticity and plasticity theory can only be successful in describing the overall behavior of materials if the largest of these microstructural length scales is considerably smaller than the scale of application. In ordered materials, this ensures that a volume which is small at the macroscopic or component scale, still contains several wavelengths of the microstructure and can therefore be modeled independently of the precise position and orientation with respect to this microstructure. In disordered materials, it contains a sufficient number of irregularities for their random effects to cancel. It is worth mentioning that similar statements can be made about time scales; however, in this contribution emphasis is on the effect of spatial scales.

When the relevant macroscopic length scale approaches the largest microstructural scale in a material, microstructural effects are no longer averaged out in the macroscopic response [1]. Note that this does not necessarily require the overall dimensions of components to be small. Even in large structures, high-frequency wave propagation or localized deformation bands may result in variations of the relevant macroscopic fields at the scale of the microstructure. In each of these situations the microstructure and its local behavior may strongly influence the observed macroscopic response. For instance, the propagation of elastic waves in crystalline materials exhibits anisotropic and dispersive effects as a result of the interaction of the waves with the crystal lattice (see, for instance, [2] and references therein). In forming operations on thin metallic strips, the distribution of plastic strain may vary significantly between specimens depending on the orientation of individual grains (see, e.g., [3]). This clearly leads to a large scatter in experiments in which the grain orientation is not controlled. Average results, however, often also show a systematic dependence on specimen size relative to, e.g., grain size. In tensile tests on thin metallic strips a decrease of the apparent strength with specimen thickness has been reported [3]. Bending and torsion tests, on the other hand, show a substantial strengthening with respect to the classical theory [4,5].

Microstructural effects can often be described accurately and in a natural way by modeling the microstructure in detail at the

dominant size scale, assuming relatively simple constitutive relations at this scale. Examples are beam-network models of metal foams, which allow one to capture the strain profiles and size effects observed in experiments [6], and discrete dislocation dynamics models, which capture the influence of hard particles in a plastically deforming metallic matrix on the yield strength [7]. Although much more efficient than atomistic simulations, these microstructural analyses are still rather expensive and provide much more detailed results than required, for instance, by design engineers. Furthermore, they require geometric and material data which may be difficult to obtain and may vary between different instances of the same product or specimen. Engineers, therefore, have a legitimate interest in continuum theories that can predict the average response (or bounds) of the real-size components taking into account the effect of microstructure, or at least the typical scale of the microstructure. Note that "average" should usually be interpreted as "ensemble average" in this context, since volume averaging may smoothen stress and strain variations to an unacceptable degree.

An interesting and promising intermediate solution is provided by multilevel finite element or computational homogenization techniques used by [8,9]; see also the contribution by Kouznetsova *et al.* [10] to this issue. These methods employ a homogeneous continuum formulation at the macroscale, but extract the constitutive response by a pointwise link with a micromechanical model, which usually consists of a finite element model on its own. Like the truly microstructural models, this approach does not require the formulation of macroscopic constitutive relations and allows one to make (usually more realistic) constitutive assumptions at a lower, microscopic scale. Connecting the two scales when they are not well separated, however, still presents a theoretical challenge [9,10]. Furthermore, due to the computational cost of the microscale finite element analyses, the method will not easily be able to compete with closed-form macroscopic theories in those cases where the latter are available.

Closed-form macroscopic continuum frameworks which take into account microstructural effects and, in particular, the relevant length scale(s) of the microstructure, have been developed since the early 1960s [11–15], although the much earlier work by the Cosserat brothers [16] should also be mentioned in this connection. The end of the previous century has shown a renaissance of these theories, which was driven by the desire to properly capture shear bands and other localized failure bands, as well as to capture size effects that were observed in experiments [17–24]. Finite element algorithms have been developed that allow one to solve the relevant equations for realistic geometries in an accurate and reliable manner [25–29]. Finite element as well as analytical solutions obtained for simple geometries generally show the desired behavior, i.e., shear bands and damage bands of a finite width and size effects that compare well with the available experiment data.

Crucial in the success of the enhanced continuum formulations is that they introduce a material length scale — or sometimes several of them [22]. It is this length that sets the width of localization bands and the size at which size effects come into play. It is generally accepted that the material length scale should be related to the typical dimensions of the relevant microstructural features. However, the precise way in which it enters the continuum formulation, although sometimes motivated by micromechanical arguments and by thermodynamical principles, is usually largely based on phenomenology. This implies that constitutive relations and the parameters featured in them must always be determined from experiments. For a number of theories and materials, such an experimental parameter identi-

fication, including that of the internal length scale, has indeed been carried out successfully (see, e.g., [4,5,30,31]). However, these identification procedures not only require advanced experimental techniques, but they also have a limited predictive power: for every new material or new microstructure new experiments are needed.

Extensive and repeated experimental identification may be avoided if a rigorous connection can be made between microstructure and its effect on the overall response. Classical homogenization methods make this connection by predicting average properties of a material (or bounds on them) based on the properties of the constituents and their geometrical arrangement (see, e.g., [32–37]). In their standard form, however, these methods fail to include the scale of the microstructure in the resulting constitutive laws. Where this scale has a significant influence on the overall response, such as in the situations discussed above, extensions of the classical theory are required.

For linear elastic random composites, an enhanced homogenization method has been proposed by Willis and coworkers [36,38,39]. A nonlocal effective representation is derived by formally solving the equilibrium equations in terms of a stress polarization and subsequent ensemble averaging. The method requires statistical data on the random microstructure. In particular, two-point statistical data introduces the typical scale of microstructural fluctuations and, thus, sets the length scale of the nonlocal effective theory. A similar path was followed before by Beran and McCoy [40,41], resulting in an effective higher-order gradient theory. Higher-order gradient theories for periodic, linear elastic media have been developed by Boutin [42] and Triantafyllidis and Bardenhagen [43] using an asymptotic solution of the microstructural problem. The size of the periodic cell enters the higher-order effective continuum as the microstructural length scale. For the simplified case of antiplane shear, Smyshlyaev and Cherednichenko [1] have refined this approach by introducing variational arguments. Their method ensures that the difference between real and homogenized behavior is minimized and that the homogenized equilibrium equations are elliptic.

In each of the above enhanced homogenization methods, closed-form expressions can only be obtained for very simple microstructures (e.g., laminates [42]). Applications to real materials require a computational strategy to solve the relevant equations. It is the objective of this contribution to develop such a computational strategy and to apply it to a two-phase composite. The method proposed by Smyshlyaev and Cherednichenko [1] is taken as a starting point for this development. It is first extended to the fully three-dimensional case in Section 2 (see also [44]). As in the antiplane shear case discussed by Smyshlyaev and Cherednichenko, a number of boundary value problems must be solved on the periodic cell in order to determine the higher-order elasticity constants of the overall strain gradient elasticity description. These problems are cast in a weak form and solved by the finite element method. Effective higher-order moduli can then be computed directly from the numerical solutions (Section 3). In Section 4, the method is applied to a matrix-inclusion system, for which the influence of the ratio of the elastic moduli of the inclusion and matrix on the effective behavior is examined.

2. HOMOGENIZATION TOWARD STRAIN GRADIENT ELASTICITY

The homogenization method developed in this paper largely follows that of Smyshlyaev and Cherednichenko [1]. However, the limitation to antiplane shear made by them is dropped. As a consequence, the scalar character of the equations is lost and vector problems must be considered. The influence of this change of charac-

ter on the main development is limited, but it may have some impact on the formal justification of the asymptotics, which is not considered here.

2.1 Heterogeneous Problem

The setting of the heterogeneous problem considered here is a simple extension to three dimensions of that of Smyshlyaev and Cherednichenko [1]; see Fig. 1 for a graphical representation of the one-dimensional case. The microstructure of the material is constructed from a unit cell $\mathbf{Q} = [0,1] \times [0,1] \times [0,1]$ by rescaling by a small parameter ε and repetition along each of the coordinates x_i ($i = 1,2,3$). The period of the material is thus $\varepsilon\mathbf{Q}$, and the parameter ε appears as the natural length scale. A body force **f(x)** is applied, which is also periodic but has a larger period $\mathbf{T} = [0,T] \times [0,T] \times [0,T]$, where T is of the order of one and T/ε is an integer; at the scale ε of the microstructure **f(x)** is assumed to be smooth. It is emphasized that the macroscopic periodicity (period $\mathbf{T}$) is used only in developing the homogenization process; the effective relations following from it can also be used in nonperiodic problems. The microscopic periodicity (period $\varepsilon\mathbf{Q}$), on the other hand, is essential for the method to work.

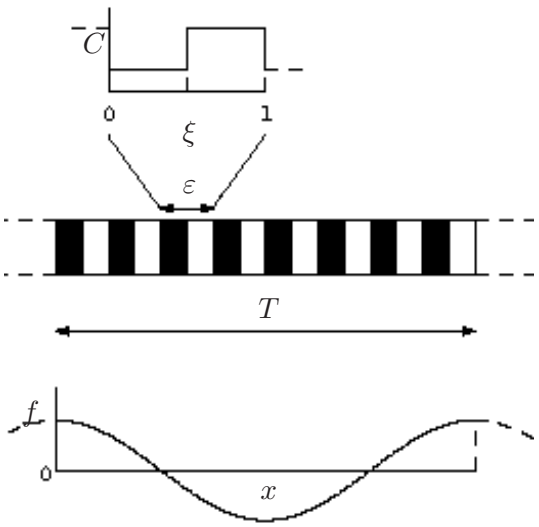

FIGURE 1. One-dimensional heterogeneous elasticity problem with double periodicity

The three-dimensional equilibrium problem on the period $\mathbf{T}$ can be written as

$$\frac{\partial \sigma_{ij}}{\partial x_i} + f_j(\mathbf{x}) = 0 \qquad (j = 1,2,3) \tag{1}$$

where the Cauchy stress tensor is given by

$$\sigma_{ij} = C_{ijkl}(\mathbf{x}/\varepsilon)\, e_{kl} \quad e_{kl} = \frac{1}{2}\left(\frac{\partial u_k}{\partial x_l} + \frac{\partial u_l}{\partial x_k}\right) \tag{2}$$

and summation is implied over the repeated indices $i,k,l = 1,2,3$. The elasticity tensor $C_{ijkl}(\boldsymbol{\xi})$ satisfies the usual symmetries $C_{ijkl} = C_{jikl} = C_{ijlk} = C_{klij}$ and is assumed to be positive-definite and piecewise smooth; the appropriate weak continuity conditions must be added to Eq. (1) at discontinuity surfaces.

Substitution of relations (2) in the set of equilibrium equations (1) results in a set of partial differential equations in terms of the displacement components $u_k(\mathbf{x})$. It proves to be useful to rewrite this set of equations in the vector form

$$\frac{\partial}{\partial x_i}\left(\mathbf{A}_{il}(\mathbf{x}/\varepsilon)\frac{\partial \mathbf{u}}{\partial x_l}\right) + \mathbf{f}(\mathbf{x}) = \mathbf{0} \tag{3}$$

where the matrix-valued functions $\mathbf{A}_{il}(\boldsymbol{\xi})$ are given in terms of the elastic moduli C_{ijkl} by $(A_{il})_{jk}(\boldsymbol{\xi}) = C_{ijkl}(\boldsymbol{\xi})$. Periodicity of the body force $\mathbf{f}$ implies that the displacement field $\mathbf{u}$ is $\mathbf{T}$-periodic; furthermore, rigid body motion is prevented by the requirement that the mean displacement on the period $\mathbf{T}$ vanishes. Together with these conditions, Eq. (3) forms a well-posed boundary value problem.

2.2 Asymptotic Solution

Equation (3) clearly shows the influence of the two scales of the problem. On the one hand, the

coefficient matrices $\mathbf{A}_{il}$ vary at the microstructural scale given by the cell size ε. On the other hand, the body force $\mathbf{f}$ has a wavelength T and is therefore related to the macroscopic scale. Homogenization methods aim at averaging the fast variations in $\mathbf{u}$, which are due to the microstructure, and at formulating equations which allow one to determine this averaged response without first solving the full, two-scale problem. Asymptotic homogenization [35,45] allows one to separate the influences of the two scales by assuming a solution of the form

$$\mathbf{u}(\mathbf{x}) = \sum_{m=0}^{\infty} \varepsilon^m \, \mathbf{u}_m(\mathbf{x}, \mathbf{x}/\varepsilon) \tag{4}$$

where the functions $\mathbf{u}_m(\mathbf{x}, \boldsymbol{\xi})$ are $\mathbf{Q}$-periodic with respect to the microstructural coordinates $\boldsymbol{\xi}$ and $\mathbf{T}$-periodic with respect to the macroscopic coordinates $\mathbf{x}$.

Straightforward substitution of Eq. (4) in Eq. (3) and requiring that the resulting equation is satisfied at each order of ε shows that the asymptotic expansion (4) must be of the form [42, 45]

$$\mathbf{u}(\mathbf{x}) = \mathbf{v}(\mathbf{x}) + \sum_{m=1}^{\infty} \varepsilon^m \sum_{|n|=m} \mathbf{N}_n(\mathbf{x}/\varepsilon) \, D^n \mathbf{v}(\mathbf{x}) \tag{5}$$

The vector-valued function $\mathbf{v}(\mathbf{x})$ is $\mathbf{T}$-periodic. Superimposed on this slowly varying field is a series of correction terms. The subscript $n = n_1 n_2 \ldots n_m$ denotes a multi-index with "length" $|n| = m$ in which each of $n_1, n_2, \ldots, n_m$ adopts the values 1, 2, 3. D^n denotes differentiation with respect to x_{n_1}, x_{n_2}, etc.: $D^n = \partial^m / \partial x_{n_1} \partial x_{n_2} \ldots \partial x_{n_m}$. So each of the correction terms in Eq. (5) consists of a derivative of $\mathbf{v}(\mathbf{x})$ modulated by a matrix-valued field $\mathbf{N}_n(\mathbf{x}/\varepsilon)$.

The functions $\mathbf{N}_n(\boldsymbol{\xi})$ are $\mathbf{Q}$-periodic and satisfy the following partial differential equation on the periodic cell [45]:

$$\frac{\partial}{\partial \xi_i} \left(\mathbf{A}_{il}(\boldsymbol{\xi}) \frac{\partial \mathbf{N}_n}{\partial \xi_l} \right) + \mathbf{T}_n(\boldsymbol{\xi}) = \mathbf{H}_n \quad (|n| = m = 1, 2, 3, \ldots) \tag{6}$$

where

$$\mathbf{T}_{n_1}(\boldsymbol{\xi}) = \frac{\partial \mathbf{A}_{in_1}}{\partial \xi_i} \qquad (m = 1) \tag{7}$$

$$\mathbf{T}_{n_1 n_2}(\boldsymbol{\xi}) = \frac{\partial}{\partial \xi_i} \left(\mathbf{A}_{in_1} \mathbf{N}_{n_2} \right) + \mathbf{A}_{n_1 l} \frac{\partial \mathbf{N}_{n_2}}{\partial \xi_l} + \mathbf{A}_{n_1 n_2} \qquad (m = 2) \tag{8}$$

$$\mathbf{T}_n(\boldsymbol{\xi}) = \frac{\partial}{\partial \xi_i} \left(\mathbf{A}_{in_1} \mathbf{N}_{n_2 \ldots n_m} \right) + \mathbf{A}_{n_1 l} \frac{\partial \mathbf{N}_{n_2 \ldots n_m}}{\partial \xi_l} + \mathbf{A}_{n_1 n_2} \mathbf{N}_{n_3 \ldots n_m} \qquad (m \geq 3) \tag{9}$$

and

$$\mathbf{H}_n = \langle \mathbf{T}_n \rangle = \int_{\mathbf{Q}} \mathbf{T}_n(\boldsymbol{\xi}) \, \mathrm{d}\boldsymbol{\xi} \tag{10}$$

Note that $\mathbf{H}_{n_1} = \mathbf{0}$ because of periodicity. Uniqueness of $\mathbf{N}_n$ is ensured by the additional requirement that their mean on the periodic cell vanishes, i.e., $\langle \mathbf{N}_n \rangle = \mathbf{0}$. Problems (6) depend only on the microstructural stiffness distribution given by $\mathbf{A}_{il}(\boldsymbol{\xi})$ and can therefore be solved independently of the macroscopic problem [in particular, independently of the distribution of body force $\mathbf{f}(\mathbf{x})$]. Since for values of $m \geq 2$ Eq. (6) depends on functions $\mathbf{N}_n$ with $|n| < m$, these problems have to be solved sequentially, for increasing m and starting at $m = 1$.

The slowly varying contribution $\mathbf{v}$ to Eq. (5) formally satisfies [45]

$$\sum_{m=2}^{\infty} \varepsilon^{m-2} \sum_{|n|=m} \mathbf{H}_n D^n \mathbf{v}(\mathbf{x}) + \mathbf{f}(\mathbf{x}) = \mathbf{0} \tag{11}$$

where $\mathbf{H}_n$ are the constant matrices defined by Eq. (10). All information on the heterogeneous

microstructure has been lumped into these matrices and only macroscopic quantities remain in Eq. (11). This equation is was, therefore, termed "homogenized equation of infinite order" by Bakhvalov and Panasenko [45], a term which will be further substantiated in the next section.

2.3 Homogenization by Ensemble Averaging

The averaged behavior of the heterogeneous material can be determined based on the argument that the precise "phase" of the microstructure with respect to the body force is generally unknown and a family of translated microstructures should therefore be considered [1]; see Fig. 2 for a one-dimensional representation. Average relations can then be obtained by ensemble averaging of the solutions for each of these translations. The translation is described by a translation vector $\boldsymbol{\zeta} \in \mathbf{Q}$; note that translations beyond $\mathbf{Q}$ need not be considered since the same periodic microstructure can always be obtained by another $\boldsymbol{\zeta} \in \mathbf{Q}$.

The equilibrium problem for a single realisation of the translation reads

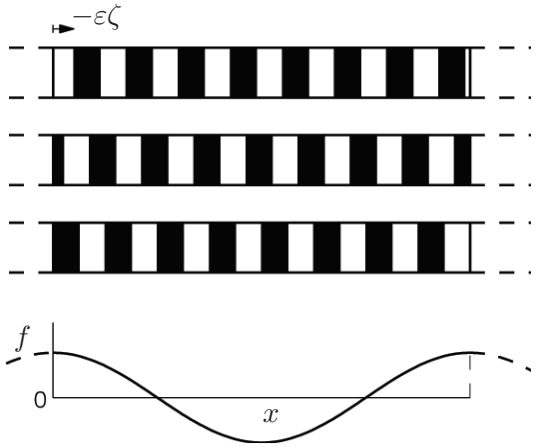

FIGURE 2. Translation of the microstructure with respect to the body force

$$\frac{\partial}{\partial x_i}\left(\mathbf{A}^{\boldsymbol{\zeta}}_{il}(\mathbf{x}/\varepsilon)\frac{\partial \mathbf{u}^{\boldsymbol{\zeta}}}{\partial x_l}\right) + \mathbf{f}(\mathbf{x}) = \mathbf{0} \qquad (12)$$

with $\mathbf{A}^{\boldsymbol{\zeta}}_{il}(\boldsymbol{\xi}) = \mathbf{A}_{il}(\boldsymbol{\xi} + \boldsymbol{\zeta})$ and the additional conditions that $\mathbf{u}^{\boldsymbol{\zeta}}$ is $\mathbf{T}$-periodic and $\langle \mathbf{u}^{\boldsymbol{\zeta}} \rangle = \mathbf{0}$. Following the same arguments that led to relation (5), it can easily be shown that the asymptotic solution to Eq. (12) is given by

$$\mathbf{u}^{\boldsymbol{\zeta}}(\mathbf{x}) = \mathbf{v}(\mathbf{x}) + \sum_{m=1}^{\infty} \varepsilon^m \sum_{|n|=m} \mathbf{N}^{\boldsymbol{\zeta}}_n(\mathbf{x}/\varepsilon)\, D^n\mathbf{v}(\mathbf{x}) \qquad (13)$$

with

$$\mathbf{N}^{\boldsymbol{\zeta}}_n(\boldsymbol{\xi}) = \mathbf{N}_n(\boldsymbol{\xi} + \boldsymbol{\zeta}) \qquad (14)$$

and $\mathbf{v}$ the same slowly varying function which appeared in Eq. (5), i.e., the solution of Eq. (11). The leading, zeroth-order term in Eq. (13) thus does not depend on the translation vector $\boldsymbol{\zeta}$, whereas the correction terms depend on $\boldsymbol{\zeta}$ in a way that is given by the translated microstructural functions $\mathbf{N}^{\boldsymbol{\zeta}}_n$ according to Eq. (14).

Expression (13) gives the asymptotic solution to the heterogeneous problem for each realization of the translated microstructure. The homogenized response is now defined as the ensemble average of this family of solutions $\mathbf{u}^{\boldsymbol{\zeta}}$:

$$\bar{\mathbf{u}}(\mathbf{x}) = \int_{\mathbf{Q}} \mathbf{u}^{\boldsymbol{\zeta}}(\mathbf{x})\, \mathrm{d}\boldsymbol{\zeta} \qquad (15)$$

Substitution of Eq. (13) results in

$$\bar{\mathbf{u}}(\mathbf{x}) = \int_{\mathbf{Q}} \mathrm{d}\boldsymbol{\zeta}\ \mathbf{v}(\mathbf{x}) + \sum_{m=1}^{\infty} \varepsilon^m \sum_{|n|=m} \int_{\mathbf{Q}} \mathbf{N}^{\boldsymbol{\zeta}}_n(\mathbf{x}/\varepsilon)\, \mathrm{d}\boldsymbol{\zeta}\ D^n\mathbf{v}(\mathbf{x}) \qquad (16)$$

where use has been made of the fact that $\mathbf{v}$ and its derivatives do not depend on $\boldsymbol{\zeta}$. The first integral on the right-hand side is equal to one because $\mathbf{Q}$ is a unit cell. Using relation (14),

the other integrals, which are associated with higher-order terms, can easily be seen to be equal to $\langle \mathbf{N}_n \rangle = \mathbf{0}$ (cf. [1]). Thus, the higher-order contributions to $\mathbf{u}^{\boldsymbol{\zeta}}$ cancel in the ensemble averaging and only the leading term $\mathbf{v}$ survives the averaging:

$$\bar{\mathbf{u}}(\mathbf{x}) = \mathbf{v}(\mathbf{x}) \tag{17}$$

This identifies the slowly varying field $\mathbf{v}$ as the true homogenized solution and Eq. (11) as the true homogenized equilibrium equation.

2.4 Truncation Based on Energetics

The above result for the homogenized equation of infinite order [i.e., Eq. (11)] is classical. However, it is not of much practical use, precisely because it is of infinite order. For practical applications it must somehow be approximated by an equation — or a system of equations — of finite order. One should realize that simply truncating the left-hand side of Eq. (11) at some order of ε may not be a good idea because ellipticity of the resulting equation cannot be guaranteed. One way to proceed has been suggested by Boutin [42] and basically means that the infinite-order equation is split into a series of second-order partial differential equations. Each of these equations has the form of an elasticity problem with a body force that depends on the solution of the previous problem. The series can be truncated to an arbitrary number of equations, thereby defining the degree of microstructural detail which is taken into account.

The approach followed by Smyshlyaev and Cherednichenko [1] is different in that it leads to a single partial differential equation — of a higher order — which has the appealing property that it falls back onto the Toupin-Mindlin strain gradient elasticity framework (see [11, 46] or Section 2.5). The finite-order governing equation is derived via a variational formulation of the averaged problem. In this way, ellipticity of the resulting equation is guaranteed in a natural way. Moreover, the resulting homogenized solution is the best possible fit to $\bar{\mathbf{u}}$ in terms of elastic energy.

The equilibrium problem for a single realization of the microstructural translation can be written in a variational form by defining on the macroscopic period $\mathbf{T}$ the energy functional

$$E^{\boldsymbol{\zeta}}[\mathbf{u}^\star] = \int_{\mathbf{T}} \left[\frac{1}{2} \left(\frac{\partial \mathbf{u}^*}{\partial x_i} \right)^{\mathrm{T}} \mathbf{A}^{\boldsymbol{\zeta}}_{il}(\mathbf{x}/\varepsilon) \, \frac{\partial \mathbf{u}^*}{\partial x_l} - \mathbf{f}^{\mathrm{T}} \mathbf{u}^* \right] \mathrm{d}\mathbf{x} \tag{18}$$

where the trial functions $\mathbf{u}^*(\mathbf{x})$ must satisfy the kinematic constraints that were imposed on the solution $\mathbf{u}^{\boldsymbol{\zeta}}$, i.e., periodicity and $\langle \mathbf{u}^* \rangle = \mathbf{0}$. The elastic energy in the equilibrium state, denoted by $I^{\boldsymbol{\zeta}}$, is the minimum of $E^{\boldsymbol{\zeta}}[\mathbf{u}^*]$ and is obtained for $\mathbf{u}^* = \mathbf{u}^{\boldsymbol{\zeta}}$:

$$I^{\boldsymbol{\zeta}} = \min_{\mathbf{u}^*(\mathbf{x})} E^{\boldsymbol{\zeta}}[\mathbf{u}^*] = E^{\boldsymbol{\zeta}}[\mathbf{u}^{\boldsymbol{\zeta}}] \tag{19}$$

Taking the ensemble average of Eq. (19) over all possible translations results in the following minimization problem for the average energy:

$$\bar{I} = \int_{\mathbf{Q}} I^{\boldsymbol{\zeta}} \mathrm{d}\boldsymbol{\zeta} = \int_{\mathbf{Q}} \min_{\mathbf{u}^*(\mathbf{x})} E^{\boldsymbol{\zeta}}[\mathbf{u}^*] \, \mathrm{d}\boldsymbol{\zeta} \tag{20}$$

Introducing the trial function $\mathbf{u}^{**}(\mathbf{x}, \boldsymbol{\zeta})$ which is $\mathbf{T}$-periodic in its first argument and $\mathbf{Q}$-periodic in its second argument, this minimization problem can be rewritten as

$$\bar{I} = \min_{\mathbf{u}^{\star\star}(\mathbf{x},\boldsymbol{\zeta})} \bar{E}[\mathbf{u}^{\star\star}] \tag{21}$$

where $\bar{E}[\mathbf{u}^{**}]$ is defined as

$$\bar{E}[\mathbf{u}^{**}] = \int_{\mathbf{Q}} E^{\boldsymbol{\zeta}}[\mathbf{u}^{**}] \, \mathrm{d}\boldsymbol{\zeta} \tag{22}$$

The minimizer of $\bar{E}[\mathbf{u}^{**}]$ clearly is $\mathbf{u}^{**}(\mathbf{x}, \boldsymbol{\zeta}) = \mathbf{u}^{\boldsymbol{\zeta}}(\mathbf{x})$, the asymptotics of which are given by Eq. (13).

The crux of the method proposed by Smyshlyaev and Cherednichenko [1] is now to restrict the set of trial functions $\mathbf{u}^{**}$ by truncating Eq. (13) after a finite number of terms. In the present three-dimensional case, this means that we consider a class $\hat{U}$ of trial functions which can be written as

$$\mathbf{u}^{**}(\mathbf{x},\boldsymbol{\zeta}) = \mathbf{v}^{*}(\mathbf{x}) + \sum_{m=1}^{K} \varepsilon^{m} \sum_{|n|=m} \mathbf{N}_{n}^{\boldsymbol{\zeta}}(\mathbf{x}/\varepsilon)\, D^{n}\mathbf{v}^{*}(\mathbf{x}) \tag{23}$$

where $K \geq 1$. A higher value of K implies that more detail of the microstructural fields is included and will result in a higher order of the resulting homogenized equations. Limiting the class of trial functions in Eq. (21) to $\hat{U}$, a minimization problem of order K can now be formulated as

$$\hat{I} = \min_{\mathbf{u}^{**}(\mathbf{x},\boldsymbol{\zeta}) \in \hat{U}} \bar{E}[\mathbf{u}^{**}] \tag{24}$$

Since the dependence of $\mathbf{u}^{**}(\mathbf{x},\boldsymbol{\zeta})$ on $\boldsymbol{\zeta}$ is known, the energy functional $\bar{E}[\mathbf{u}^{**}]$ can be rewritten solely in terms of the slowly varying field $\mathbf{v}^{*}(\mathbf{x})$ for $\mathbf{u}^{**}(\mathbf{x},\boldsymbol{\zeta}) \in \hat{U}$:

$$\hat{I} = \min_{\mathbf{v}^{*}(\mathbf{x})} \hat{E}[\mathbf{v}^{*}] \tag{25}$$

where $\hat{E}[\mathbf{v}^{*}]$ follows by substitution of Eq. (23) into Eq. (22) and use of relation (14) as

$$\hat{E}[\mathbf{v}^{*}] = \int_{\mathbf{T}} \begin{bmatrix} \sum_{r,s=1}^{K+1} \varepsilon^{r+s-2} \\ \sum_{|p|=r,|q|=s} \tfrac{1}{2} (D^{p}\mathbf{v}^{*})^{\mathrm{T}} \hat{\mathbf{H}}_{p;q} \\ D^{q}\mathbf{v}^{*} - \mathbf{f}^{\mathrm{T}}\mathbf{v}^{*} \end{bmatrix} \mathrm{d}\mathbf{x} \tag{26}$$

with

$$\begin{aligned} \hat{\mathbf{H}}_{p;q} &= \int_{\mathbf{Q}} \left(\frac{\partial \mathbf{N}_{p}}{\partial \xi_{i}} + \delta_{ip_1} \mathbf{N}_{p_2 \ldots p_r} \right)^{\mathrm{T}} \\ &\times \mathbf{A}_{il}(\boldsymbol{\xi}) \left(\frac{\partial \mathbf{N}_{q}}{\partial \xi_{l}} + \delta_{lq_1} \mathbf{N}_{q_2 \ldots q_s} \right) \mathrm{d}\boldsymbol{\xi} \\ &(r,s = 2,\ldots,K) \end{aligned} \tag{27}$$

For $r = 1$ or $s = 1$, the factors $\mathbf{N}_{p_2 \ldots p_r}$ or $\mathbf{N}_{q_2 \ldots q_s}$ in Eq. (27) must be replaced by the identity matrix $\mathbf{I}$; for $r = K+1$ or $s = K+1$ the terms $\partial \mathbf{N}_{p}/\partial x_{i}$ or $\partial \mathbf{N}_{q}/\partial x_{l}$ must be dropped, respectively. The constant matrices $\hat{\mathbf{H}}_{p;q}$ can be computed solely on the basis of the microstructural stiffness distribution and the microstructural functions $\mathbf{N}_{n}$, and can therefore be determined independently of the macroscopic problem.

Limiting the energy minimization to trial functions $\mathbf{u}^{**} \in \hat{U}$ for which the microstructural influence is given by Eq. (23) implies that the energy $\hat{I}$ obtained in this minimization will generally be higher than the true mean energy $\bar{I}$. Furthermore, the minimizer $\hat{\mathbf{v}}$ of $\hat{E}[\mathbf{v}^{*}]$ generally will not satisfy the homogenized equation of infinite order (11). The elastic energy $\hat{I}$ generated by this minimiser, however, is the closest possible to $\bar{I}$ within the limited class of trial functions. In this sense, $\hat{\mathbf{v}}$ is the best possible approximation of $\mathbf{v}$ for a given order K of the microstructural influence in Eq. (23); it was, therefore, termed "homogenized solution of order K" by Smyshlyaev and Cherednichenko [1]. The "homogenized equation of order K," i.e., the truncated counterpart of Eq. (11), which is satisfied by $\hat{\mathbf{v}}$, can be obtained as the Euler-Lagrange equation associated with the minimization (25). This equation can be interpreted as an equilibrium problem for a grade-n elastic medium (see [44]). Here, however, Smyshlyaev and Cherednichenko's interpretation as a strain gradient continuum in the sense of Toupin and Mindlin [11,46] is followed.

2.5 Interpretation in Terms of Strain Gradient Elasticity

The strain gradient continuum theory due to Toupin and Mindlin [11,46] is a generalization of standard continuum mechanics in the sense that, apart from the usual first-order gradients of displacement (i.e., strain), higher-order gradients of the displacement are also taken into account in the kinematics — in principle to an arbitrary order. For instance, in the theory developed in [46], gradients up to order 3 are considered. Each of these deformation measures has a higher-order stress measure associated with it, which is work conjugate to it. The equilibrium equations that must be satisfied by these higher-order stresses and constitutive relations between stresses and (higher-order) strains have been derived from an energy potential via variational considerations (see, e.g., [46]).

In a similar fashion, effective constitutive relations of the strain gradient type can be retrieved from the energy minimization problem (25) by casting it in a variational form. Using the symmetry property $\hat{\mathbf{H}}_{p;q} = \hat{\mathbf{H}}^{\mathrm{T}}_{q;p}$, the variation $\delta\hat{E}$ due to a variation $\delta\mathbf{v}^*$ of the trial function $\mathbf{v}^*$ can be written as

$$\delta\hat{E} = \int_{\mathbf{T}} \left[\begin{array}{l} \displaystyle\sum_{r=1}^{K+1} \sum_{|p|=r} \left(D^p \delta\mathbf{v}^*\right)^{\mathrm{T}} \\ \displaystyle\times \left(\sum_{s=1}^{K+1} \varepsilon^{r+s-2} \right. \\ \displaystyle\left. \sum_{|q|=s} \hat{\mathbf{H}}_{p;q}\, D^q \mathbf{v}^* \right) - \delta\mathbf{v}^{*\mathrm{T}} \mathbf{f} \end{array} \right] \mathrm{d}\mathbf{x} \quad (28)$$

The factors $D^p\delta\mathbf{v}^*$ in the kernel of the integral can be recognised as variations of the higher-order deformation gradients

$$e^*_{pj} = D^p v^*_j \qquad (|p| = r \geq 2) \quad (29)$$

associated with the slow displacement variation $\mathbf{v}^*$; the first-order gradient terms can be symmetrized in the usual way

$$e^*_{p_1 j} = \frac{1}{2}\left(\frac{\partial v^*_j}{\partial x_{p_1}} + \frac{\partial v^*_{p_1}}{\partial x_j} \right) \quad (|p| = r = 1) \quad (30)$$

Using these expressions and the minor symmetries of $\hat{\mathbf{H}}_{p;q}$, Eq. (28) can be rewritten as

$$\delta\hat{E} = \int_{\mathbf{T}} \left[\sum_{r=1}^{K+1} \sum_{|p|=r} \delta e^*_{pj} \sigma^*_{pj} - \delta v^*_j f_j \right] \mathrm{d}\mathbf{x} \quad (31)$$

where the terms between round brackets in Eq. (28) have been identified as the higher-order stresses conjugate to δe^*_{pj}:

$$\sigma^*_{pj} = \sum_{s=1}^{K+1} \varepsilon^{|p|+s-2} \sum_{|q|=s} \hat{C}_{pj;qk} e^*_{qk} \quad (32)$$

with

$$\hat{C}_{pj;qk} = \frac{1}{|p|!|q|!} \sum_{\substack{p'=\mathcal{P}(p) \\ q'=\mathcal{P}(q)}} \left(\hat{H}_{p';q'} \right)_{jk} \quad (33)$$

and $\mathcal{P}(p)$ denoting all possible permutations of p. Note that the stiffness coefficients $\hat{C}_{pj;qk}$ have been symmetrized with respect to p and q in order to reduce the number of independent values.

Integration by parts and realising that the resulting boundary terms vanish because of periodicity allows to rewrite Eq. (31) as

$$\delta\hat{E} = -\int_{\mathbf{T}} \delta v^*_j \left[\sum_{r=1}^{K+1} (-1)^{r-1} \sum_{|p|=r} D^p \sigma^*_{pj} + f_j \right] \mathrm{d}\mathbf{x} \quad (34)$$

Now, for the energy minimizer $\hat{\mathbf{v}}$ and the stresses $\hat{\sigma}_{pj}$ associated with it, the variation $\delta\hat{E}$

must vanish for all admissible δv_j^*. The above expression for $\delta \hat{E}$ shows that this can only be true if

$$\sum_{r=1}^{K+1}(-1)^{r-1}\sum_{|p|=r} D^p \hat{\sigma}_{pj} + f_j = 0 \quad (j = 1, 2, 3) \quad (35)$$

These equations are exactly the equilibrium equations of the Toupin-Mindlin framework, formulated in terms of the effective (higher-order) stresses associated with the homogenized solution $\hat{\mathbf{v}}$. Indeed, it can easily be verified that for $K = 0$ they reduce to the standard equilibrium equations of classical continuum mechanics. If more microstructural effects are taken into account in Eq. (23), i.e., for $K \geq 1$, higher-order stresses come into play and the order of the equations becomes $K + 1$ in terms of these stresses. For $K = 1$ only second-order displacement gradients (or gradients of strain) and so-called double stresses appear [11,12]; this is also the case which was extended to plasticity by Fleck and Hutchinson [22]. For $K = 2$ the theory of [46] is retrieved and even higher K lead to the natural extensions of these cases to higher orders.

The above shows that an effective strain gradient description is obtained as the natural outcome of homogenizing a standard elastic medium. Perhaps more importantly, it also shows how to determine the effective constitutive behavior of the heterogeneous material in terms of higher-order strains and stresses. For the homogenized solution $\hat{\mathbf{v}}$ the homogenized deformation gradients according to Eqs. (29)–(30) become

$$\hat{e}_{q_1 k} = \frac{1}{2}\left(\frac{\partial \hat{v}_k}{\partial x_{q_1}} + \frac{\partial \hat{v}_{q_1}}{\partial x_k}\right) \quad (|q| = s = 1) \quad (36)$$

$$\hat{e}_{qk} = D^q \hat{v}_k \quad (|q| = s \geq 2) \quad (37)$$

and the homogenized stresses generated by this deformation read [cf. (32)]

$$\hat{\sigma}_{pj} = \sum_{s=1}^{K+1} \varepsilon^{|p|+s-2} \sum_{|q|=s} \hat{C}_{pj;qk}\hat{e}_{qk} \quad (38)$$

where the constants $\hat{C}_{pj;qk}$ are given by Eq. (33). These constants should be compared to the standard elastic moduli of linear elasticity; together with the constitutive relations (38), they uniquely define the higher-order effective response of the heterogeneous material. Relations (38) also show that the periodic cell size ε, which is the typical length scale of the microstructure, enters the effective constitutive relations. The effective properties are, therefore, clearly size dependent, and macroscopic analyses using these properties will show a size effect as the macroscopic dimensions are diminished to the order of the microstructural size ε. The precise influence of the material length scale in different directions is governed by the elastic moduli $\hat{C}_{pj;qk}$ and may therefore be highly anisotropic.

It is emphasised that the moduli $\hat{C}_{pj;qk}$ are not unknown parameters, but can be computed in a systematic way for any periodic microstructure once the cell problems given by Equation (6) have been solved. The resulting microstructural fields $\mathbf{N}_n(\boldsymbol{\xi})$ can then be inserted in (27), after which the moduli $\hat{C}_{pj;qk}$ can be determined via Eq. (33). Particularly for higher orders, a substantial amount of data can thus be generated, for which it is difficult to imagine how it could be determined purely experimentally. It is worth mentioning in this connection that already for an isotropic, second-order linear elastic strain gradient theory, 18 independent elastic constants were identified in [46]. It needs no further explanation that this number increases dramatically if anisotropy is considered and as the framework is extended to higher orders.

3. FINITE ELEMENT IMPLEMENTATION

A crucial step in determining the effective higher-order response of the heterogeneous material, characterized by the moduli $\hat{C}_{pj;qk}$ as discussed above, consists in solving the microstructural boundary value problems given by Eq. (6) together with Eqs. (7)–(9) and the conditions of periodicity and vanishing average. As was stated before, these problems are fully determined by the microstructure of the material and can therefore be solved independently of the macroscopic problem at hand. For relatively simple microstructures, they can be solved analytically (see, for instance, Boutin [42] for the case of a two-phase laminate). For less trivial geometric arrangements, a numerical approach must be followed. In this contribution, a finite element algorithm is developed for this purpose.

Given the dependence of the terms $\mathbf{T}_n$ and $\mathbf{H}_n$ in Eq. (6) for a certain order $m = |n|$ on the functions $\mathbf{N}_n$ of order $m-1$ and lower, the microstructural problems must be solved for increasing order m. At a certain order, Eq. (6) can be regarded as a set of linear elasticity equations, with each column of $\mathbf{T}_n - \mathbf{H}_n$ representing a body force vector, which is known once all problems of lower order have been solved. The columns of $\mathbf{N}_n$ are then the displacement fields corresponding to these body forces. The development of the finite element algorithm to solve these equations is therefore largely parallel to that for boundary value problems in linear elasticity. Instead of the usual displacement or traction boundary conditions, however, the solutions of Eq. (6) must satisfy $\mathbf{Q}$-periodicity and have mean zero. The latter condition can easily be dealt with by first solving the problem with $\mathbf{N}_n$ fixed at the corners of the cell and, subsequently, subtracting from this solution its average. Periodicity can be enforced by introducing dependencies between the boundary nodes of the finite element discretization (see also below).

3.1 Weak Formulation of Cell Problems

The finite element discretization of cell problems is based on the weak form of Eq. (6). This weak form is first derived for the case $m \geq 3$ using the weighted residuals formalism. After substitution of $\mathbf{T}_n(\boldsymbol{\xi})$ according to Eq. (9), Eq. (6) reads

$$\frac{\partial}{\partial \xi_i}\left(\mathbf{A}_{il}\frac{\partial \mathbf{N}_n}{\partial \xi_l}\right) + \frac{\partial}{\partial \xi_i}\left(\mathbf{A}_{in_1}\mathbf{N}_{n_2\ldots n_m}\right) + \mathbf{A}_{n_1 l}\frac{\partial \mathbf{N}_{n_2\ldots n_m}}{\partial \xi_l} + \mathbf{A}_{n_1 n_2}\mathbf{N}_{n_3\ldots n_m} = \mathbf{H}_n \quad (39)$$

Multiplication of this equation by a $\mathbf{Q}$-periodic, vector-valued test function $\boldsymbol{\psi}(\mathbf{x})$ and integration over the cell $\mathbf{Q}$ results in the weighted residuals form

$$\begin{aligned}&\int_{\mathbf{Q}} \boldsymbol{\psi}^{\mathrm{T}}\frac{\partial}{\partial \xi_i}\left(\mathbf{A}_{il}\frac{\partial \mathbf{N}_n}{\partial \xi_l}\right)\mathrm{d}\boldsymbol{\xi} \\ &+ \int_{\mathbf{Q}} \boldsymbol{\psi}^{\mathrm{T}}\frac{\partial}{\partial \xi_i}(\mathbf{A}_{in_1}\mathbf{N}_{n_2\ldots n_m})\mathrm{d}\boldsymbol{\xi} \\ &+ \int_{\mathbf{Q}} \boldsymbol{\psi}^{\mathrm{T}}\mathbf{A}_{n_1 l}\frac{\partial \mathbf{N}_{n_2\ldots n_m}}{\partial \xi_l}\,\mathrm{d}\boldsymbol{\xi} \\ &+ \int_{\mathbf{Q}} \boldsymbol{\psi}^{\mathrm{T}}\mathbf{A}_{n_1 n_2}\mathbf{N}_{n_3\ldots n_m}\,\mathrm{d}\boldsymbol{\xi} = \int_{\mathbf{Q}} \boldsymbol{\psi}^{\mathrm{T}}\mathbf{H}_n\,\mathrm{d}\boldsymbol{\xi} \quad (40)\end{aligned}$$

which must be satisfied for all admissible $\boldsymbol{\psi}$. The continuity conditions on $\mathbf{N}_n$ can be relaxed by integration by parts of the first two integrals; after reordering this yields the weak formulation

$$\int_{\mathbf{Q}} \frac{\partial \boldsymbol{\psi}}{\partial \xi_i}^{\mathrm{T}} \mathbf{A}_{il} \frac{\partial \mathbf{N}_n}{\partial \xi_l} \, \mathrm{d}\boldsymbol{\xi} =$$
$$- \int_{\mathbf{Q}} \frac{\partial \boldsymbol{\psi}}{\partial \xi_i}^{\mathrm{T}} \mathbf{A}_{in_1} \mathbf{N}_{n_2 \ldots n_m} \, \mathrm{d}\boldsymbol{\xi}$$
$$+ \int_{\mathbf{Q}} \boldsymbol{\psi}^{\mathrm{T}} \mathbf{A}_{n_1 l} \frac{\partial \mathbf{N}_{n_2 \ldots n_m}}{\partial \xi_l} \, \mathrm{d}\boldsymbol{\xi}$$
$$+ \int_{\mathbf{Q}} \boldsymbol{\psi}^{\mathrm{T}} \mathbf{A}_{n_1 n_2} \mathbf{N}_{n_3 \ldots n_m} \, \mathrm{d}\boldsymbol{\xi}$$
$$- \int_{\mathbf{Q}} \boldsymbol{\psi}^{\mathrm{T}} \mathbf{H}_n \, \mathrm{d}\boldsymbol{\xi} \tag{41}$$

Note that the boundary terms which result from the integration by parts, vanish because of periodicity.

It is now convenient to condense the summation over i and l in Eq. (41) into matrix form. To this end the following 9×1 matrices are defined:

$$\mathbf{D}\boldsymbol{\psi} = \begin{bmatrix} \dfrac{\partial \boldsymbol{\psi}}{\partial \xi_1} \\ \dfrac{\partial \boldsymbol{\psi}}{\partial \xi_2} \\ \dfrac{\partial \boldsymbol{\psi}}{\partial \xi_3} \end{bmatrix} \qquad \mathbf{D}\mathbf{N}_n = \begin{bmatrix} \dfrac{\partial \mathbf{N}_n}{\partial \xi_1} \\ \dfrac{\partial \mathbf{N}_n}{\partial \xi_2} \\ \dfrac{\partial \mathbf{N}_n}{\partial \xi_3} \end{bmatrix} \tag{42}$$

as well as the 9×9 and 9×3 matrices

$$\mathbf{A} = \begin{bmatrix} \mathbf{A}_{11} & \mathbf{A}_{12} & \mathbf{A}_{13} \\ \mathbf{A}_{21} & \mathbf{A}_{22} & \mathbf{A}_{23} \\ \mathbf{A}_{31} & \mathbf{A}_{32} & \mathbf{A}_{33} \end{bmatrix} \qquad \mathbf{A}_{n_1} = \begin{bmatrix} \mathbf{A}_{1n_1} \\ \mathbf{A}_{2n_1} \\ \mathbf{A}_{3n_1} \end{bmatrix} \tag{43}$$

With these definitions, Eq. (41) can be rewritten as

$$\int_{\mathbf{Q}} (\mathbf{D}\boldsymbol{\psi})^{\mathrm{T}} \mathbf{A} \, \mathbf{D}\mathbf{N}_n \, \mathrm{d}\boldsymbol{\xi} =$$
$$- \int_{\mathbf{Q}} (\mathbf{D}\boldsymbol{\psi})^{\mathrm{T}} \mathbf{A}_{n_1} \mathbf{N}_{n_2 \ldots n_m} \, \mathrm{d}\boldsymbol{\xi}$$
$$+ \int_{\mathbf{Q}} \boldsymbol{\psi}^{\mathrm{T}} \mathbf{A}_{n_1}^{\mathrm{T}} \mathbf{D}\mathbf{N}_{n_2 \ldots n_m} \, \mathrm{d}\boldsymbol{\xi}$$
$$+ \int_{\mathbf{Q}} \boldsymbol{\psi}^{\mathrm{T}} \mathbf{A}_{n_1 n_2} \mathbf{N}_{n_3 \ldots n_m} \, \mathrm{d}\boldsymbol{\xi}$$
$$- \int_{\mathbf{Q}} \boldsymbol{\psi}^{\mathrm{T}} \mathbf{H}_n \, \mathrm{d}\boldsymbol{\xi} \tag{44}$$

Note that the matrix products can, in principle, be condensed slightly further using the symmetries of $\mathbf{A}_{il}$ (cf. standard elasticity); however, this is not done here for clarity.

The equivalents of Eq. (44) for $m = 1$ and $m = 2$ follow analogically. The result for $m = 2$ can be obtained from Eq. (44) by dropping the factor $\mathbf{N}_{n_3 \ldots n_m}$ in the third term on the right-hand side. Likewise, for $m = 1$, the factor $\mathbf{N}_{n_2 \ldots n_m}$ disappears in the first right-hand side term; all other terms on the right-hand side disappear entirely.

3.2 Discretization by Finite Element Shape Functions

The weak forms obtained above can now be discretized by interpolating the test function $\boldsymbol{\psi}(\boldsymbol{\xi})$ and the microstructural functions $\mathbf{N}_n(\boldsymbol{\xi})$ in the standard way

$$\boldsymbol{\psi}(\boldsymbol{\xi}) = \boldsymbol{\Phi}(\boldsymbol{\xi}) \tilde{\boldsymbol{\psi}} \qquad \mathbf{N}_n(\boldsymbol{\xi}) = \boldsymbol{\Phi}(\boldsymbol{\xi}) \tilde{\mathbf{N}}_n \tag{45}$$

where $\boldsymbol{\Phi}(\boldsymbol{\xi})$ contains the finite element interpolation functions and the vector $\tilde{\boldsymbol{\psi}}$ and the matrix $\tilde{\mathbf{N}}_n$ contain the nodal components of $\boldsymbol{\psi}$ and $\mathbf{N}_n$, respectively. Using the same interpolation, the derivatives $\mathbf{D}\boldsymbol{\psi}$ and $\mathbf{D}\mathbf{N}_n$ can be written as

$$\mathbf{D}\boldsymbol{\psi}(\boldsymbol{\xi}) = \mathbf{B}(\boldsymbol{\xi}) \tilde{\boldsymbol{\psi}} \qquad \mathbf{D}\mathbf{N}_n(\boldsymbol{\xi}) = \mathbf{B}(\boldsymbol{\xi}) \tilde{\mathbf{N}}_n \tag{46}$$

where $\mathbf{B}(\xi)$ contains the shape function derivatives. The microstructural functions of lower order will generally have been computed using the same discretization and are therefore available in the same discrete form given by Eqs. (45)–(46).

Substitution of the respective discretizations in Eq. (44) and realizing that the resulting equation must be satisfied for all $\tilde{\psi}$ results in a set of discrete equations of the form

$$\mathbf{K}\,\tilde{\mathbf{N}}_n = \mathbf{F}_n \tag{47}$$

where $\mathbf{K}$ is the standard stiffness matrix in elasticity, given by

$$\mathbf{K} = \int_{\mathbf{Q}} \mathbf{B}^{\mathrm{T}}\mathbf{A}\,\mathbf{B}\,\mathrm{d}\boldsymbol{\xi} \tag{48}$$

and $\mathbf{F}_n$ is a matrix, which reads

$$\begin{aligned}\mathbf{F}_n = &- \int_{\mathbf{Q}} \mathbf{B}^{\mathrm{T}}\mathbf{A}_{n_1}\boldsymbol{\Phi}\,\mathrm{d}\boldsymbol{\xi}\tilde{\mathbf{N}}_{n_2\ldots n_m} \\ &+ \int_{\mathbf{Q}} \boldsymbol{\Phi}^{\mathrm{T}}\mathbf{A}_{n_1}^{\mathrm{T}}\mathbf{B}\,\mathrm{d}\boldsymbol{\xi}\,\tilde{\mathbf{N}}_{n_2\ldots n_m} \\ &+ \int_{\mathbf{Q}} \boldsymbol{\Phi}^{\mathrm{T}}\mathbf{A}_{n_1n_2}\boldsymbol{\Phi}\,\mathrm{d}\boldsymbol{\xi}\,\tilde{\mathbf{N}}_{n_3\ldots n_m} \\ &- \int_{\mathbf{Q}} \boldsymbol{\Phi}^{\mathrm{T}}\mathbf{H}_n\,\mathrm{d}\boldsymbol{\xi} \qquad (m \geq 3)\end{aligned} \tag{49}$$

The matrix $\mathbf{H}_n$ in this expression can be computed from Eqs. (9) and (10) on the basis of the numerical solutions obtained at lower orders

$$\begin{aligned}\mathbf{H}_n = &\int_{\mathbf{Q}} \mathbf{A}_{n_1}^{\mathrm{T}}\mathbf{B}\,\mathrm{d}\boldsymbol{\xi}\,\tilde{\mathbf{N}}_{n_2\ldots n_m} \\ &+ \int_{\mathbf{Q}} \mathbf{A}_{n_1n_2}\boldsymbol{\Phi}\,\mathrm{d}\boldsymbol{\xi}\,\tilde{\mathbf{N}}_{n_3\ldots n_m} \quad (m \geq 3)\end{aligned} \tag{50}$$

Note that the first term in Eq. (9) vanishes after integration as a result of periodicity.

The discretized equations for $m = 1$ and $m = 2$ follow completely analogically. This results in systems of equations of the same form (47), but with different right-hand sides, namely,

$$\mathbf{F}_{n_1} = -\int_{\mathbf{Q}} \mathbf{B}^{\mathrm{T}}\mathbf{A}_{n_1}\,\mathrm{d}\boldsymbol{\xi} \qquad (m = 1) \tag{51}$$

and

$$\begin{aligned}\mathbf{F}_{n_1n_2} = &- \int_{\mathbf{Q}} \mathbf{B}^{\mathrm{T}}\mathbf{A}_{n_1}\boldsymbol{\Phi}\,\mathrm{d}\boldsymbol{\xi}\,\tilde{\mathbf{N}}_{n_2} \\ &+ \int_{\mathbf{Q}} \boldsymbol{\Phi}^{\mathrm{T}}\mathbf{A}_{n_1}^{\mathrm{T}}\mathbf{B}\,\mathrm{d}\boldsymbol{\xi}\,\tilde{\mathbf{N}}_{n_2} \\ &+ \int_{\mathbf{Q}} \boldsymbol{\Phi}^{\mathrm{T}}\mathbf{A}_{n_1n_2}\,\mathrm{d}\boldsymbol{\xi} \\ &- \int_{\mathbf{Q}} \boldsymbol{\Phi}^{\mathrm{T}}\mathbf{H}_{n_1n_2}\,\mathrm{d}\boldsymbol{\xi} \qquad (m = 2)\end{aligned} \tag{52}$$

In the latter expression, the matrix $\mathbf{H}_{n_1n_2}$ can be evaluated as [cf. (50)]

$$\mathbf{H}_{n_1n_2} = \int_{\mathbf{Q}} \mathbf{A}_{n_1}^{\mathrm{T}}\mathbf{B}\,\mathrm{d}\boldsymbol{\xi}\,\tilde{\mathbf{N}}_{n_2} + \int_{\mathbf{Q}} \mathbf{A}_{n_1n_2}\,\mathrm{d}\boldsymbol{\xi} \quad (m = 2) \tag{53}$$

Before the linear system of Eq. (47) can be solved, periodicity of the finite element discretization must be enforced by tying the degrees of freedom associated with opposite faces of the cell to each other. Furthermore, the nodal values in the corner nodes are set equal to zero. After condensing the linear system accordingly and solving for the unknown $\tilde{\mathbf{N}}_n$, the average

$$\langle \mathbf{N}_n \rangle = \int_{\mathbf{Q}} \boldsymbol{\Phi}\,\mathrm{d}\boldsymbol{\xi}\,\tilde{\mathbf{N}}_n \tag{54}$$

is subtracted from the numerical solution in order to ensure that $\langle \mathbf{N}_n \rangle = \mathbf{0}$, see [47] for more details.

3.3 Evaluation of Elastic Moduli

Once the discretized microstructural fields $\tilde{\mathbf{N}}_n$ have been determined for all relevant orders $m \leq K$, the matrices $\hat{\mathbf{H}}_{p;q}$ can be determined from the discretized equivalent of Eq. (27)

$$\hat{\mathbf{H}}_{p;q} = \tilde{\mathbf{N}}_p^{\mathrm{T}} \int_{\mathbf{Q}} \mathbf{B}^{\mathrm{T}} \mathbf{A}\, \mathbf{B}\, \mathrm{d}\boldsymbol{\xi}\, \tilde{\mathbf{N}}_q + \tilde{\mathbf{N}}_p^{\mathrm{T}} \int_{\mathbf{Q}} \mathbf{B}^{\mathrm{T}} \mathbf{A}_{q_1}\, \boldsymbol{\Phi}\, \mathrm{d}\boldsymbol{\xi}\, \tilde{\mathbf{N}}_{q_2 \ldots q_s} + \tilde{\mathbf{N}}_{p_2 \ldots p_r}^{\mathrm{T}} \int_{\mathbf{Q}} \boldsymbol{\Phi}^{\mathrm{T}} \mathbf{A}_{p_1}^{\mathrm{T}}\, \mathbf{B}\, \mathrm{d}\boldsymbol{\xi}\, \tilde{\mathbf{N}}_q + \tilde{\mathbf{N}}_{p_2 \ldots p_r}^{\mathrm{T}} \int_{\mathbf{Q}} \boldsymbol{\Phi}^{\mathrm{T}} \mathbf{A}_{p_1 q_1}\, \boldsymbol{\Phi}\, \mathrm{d}\boldsymbol{\xi}\, \tilde{\mathbf{N}}_{q_2 \ldots q_s} \quad (m \geq 3) \quad (55)$$

for $m = 1$ and $m = K+1$ some trivial modifications again have to be made to this expression [see below Eq. (27)]. The strain gradient moduli $\hat{C}_{pj;qk}$ are now readily computed according to (33).

4. APPLICATION TO A MATRIX-INCLUSION SYSTEM

The numerical algorithms developed in the previous section have been applied to a two-dimensional microstructure, which consists of hard inclusions embedded in a softer, continuous matrix phase. The inclusions have a circular shape and are stacked in a square pattern; the periodic cell that can be distinguished in this microstructure is depicted in Fig. 3(a). The size of the inclusions is such that their volume fraction equals 0.25. Plane deformations are assumed, i.e., displacements in the direction perpendicular to the plane of the cell, are neglected. In the reference computation, Young's modulus of the inclusion E_{i} was set to 100 times that of the matrix E_{m}; this ratio has also been varied, however, in order to examine the influence of stiffness contrast between the two phases on the computed effective moduli. The Poisson ratios of the two materials equal $\nu_{\mathrm{i}} = \nu_{\mathrm{m}} = \frac{1}{3}$.

The finite element mesh which was used in the computations is shown in Figure 3(b); it consists of 2520 eight-node elements which are integrated by a reduced, four-point Gauss scheme. Higher-order gradients are taken into account up to an order of $K = 2$. This means that the effective kinematics are described by strains, second-order displacement gradients and third-order displacement gradients; apart from stresses, also double stresses and triple stresses enter the effective constitutive description. Note that this is precisely the case consider in [46].

Figure 4 shows two components of the microstructural (matrix-valued) fields $\mathbf{N}_1$ as com-

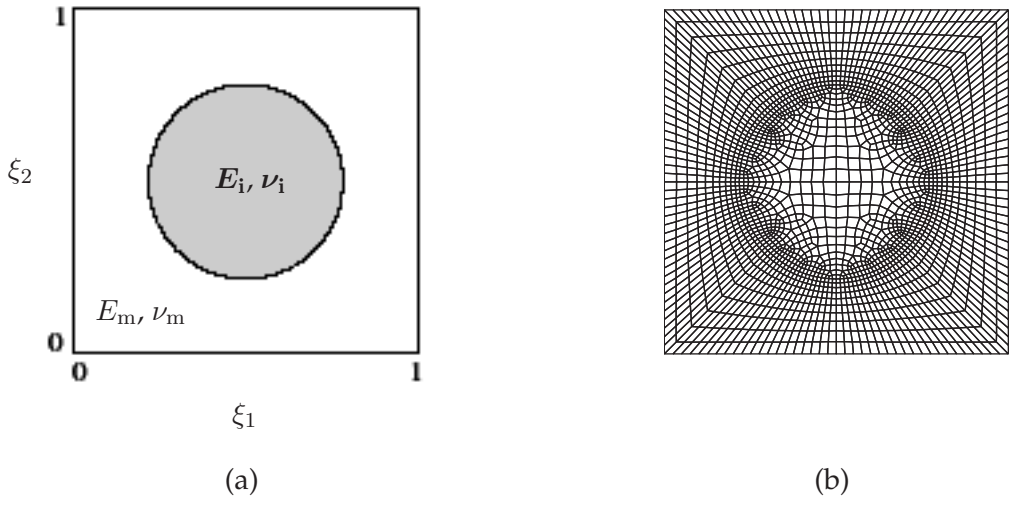

FIGURE 3. Periodic cell of the matrix-inclusion system: **(a)** geometry and **(b)** finite element discretization

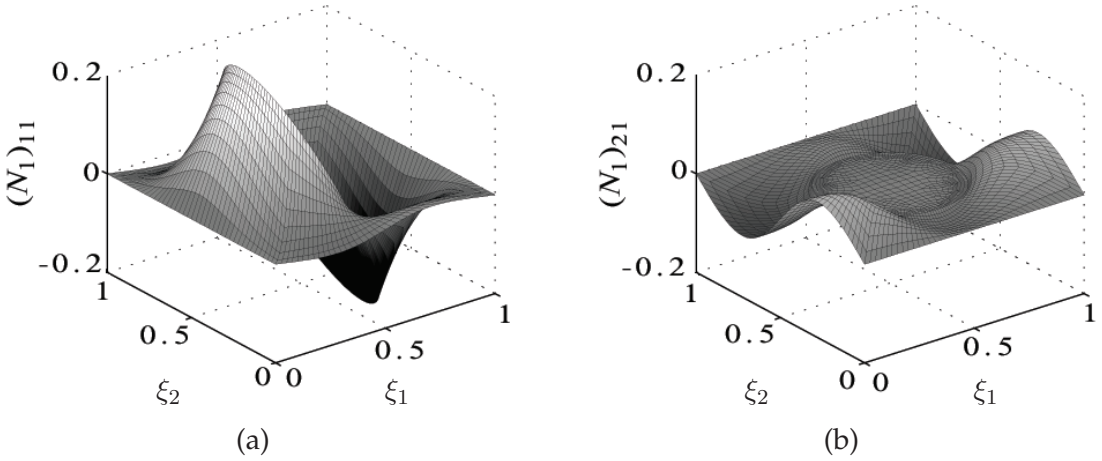

FIGURE 4. Microstructural function $\mathbf{N}_1$ computed in the first-order problems: **(a)** 11-component $(N_1)_{11}$ and **(b)** 21-component $(N_1)_{21}$

puted with the finite element algorithm for a stiffness contrast of $E_\mathrm{i}/E_\mathrm{m} = 100$; the coordinates ξ_1 and ξ_2 used in these plots have been indicated in Fig. 3(a). These functions must be interpreted as (the 1- and 2-component of) the first-order microstructural corrections to the overall displacement field as triggered by the overall (11-component of) strain [see Eq. (5)]. For instance, the negative gradient of $(N_1)_{11}$ in the part of the domain that is occupied by the fiber (Fig. 6(a)) indicates that the true, microstructural strain e_{11} in the fiber will be considerably smaller than the effective strain $\hat{e}_{11}$; in the matrix, on the other hand, it is larger than the effective strain. The $(N_1)_{21}$-field in Fig. 4(b), shows that overall straining in the 11-direction results in hardly any displacement in the ξ_2 direction within the fiber, but some rearrangement in the matrix material. Similar conclusions can be drawn for the other directions involved. Indeed, as can be seen from the double symmetry of the unit cell, the effective stiffness of the cell is orthotropic with identical properties in the two coordinate directions.

The dominant components of the solutions of the second-order problems ($m = 2$), have been plotted in Fig. 5. The 11-component of $\mathbf{N}_{11}$ [Fig. 5(a)] represents a microstructural displacement in the direction of ξ_1 under the influence of the effective displacement gradient $\hat{e}_{111} = \partial^2 \hat{v}_1 / \partial x_1^2$. Likewise, the 11-component of $\mathbf{N}_{22}$ depicted in Fig. 5(b) represents the microstructural response to an effective displacement gradient $\hat{e}_{221} = \partial^2 \hat{v}_1 / \partial x_2^2$. Both of these fields, and indeed all other fields of the same order, are smoother and also smaller in amplitude than those resulting from the first-order problem; this trend seems to persist for higher orders. It should be noted that they are furthermore multiplied by the small parameter ε (or ε^m for higher orders) when entering the asymptotic expansion (5).

The numerical representations of the microstructural fields $\mathbf{N}_n$ have been used to compute the higher-order effective stiffness moduli $\hat{C}_{pj;qk}$ by the method described in Section 3.3. Table 1 gives the resulting moduli for a stiffness contrast of $E_\mathrm{i}/E_\mathrm{m} = 100$. The values have been normalized with respect to E_m and (where appropriate) unit length. Only nonvanishing values and values that do not follow from symmetry arguments are given. The standard components $C_{p_1 j;q_1 k}$ coincide with the ones given by classical homogenization. Note that the higher-

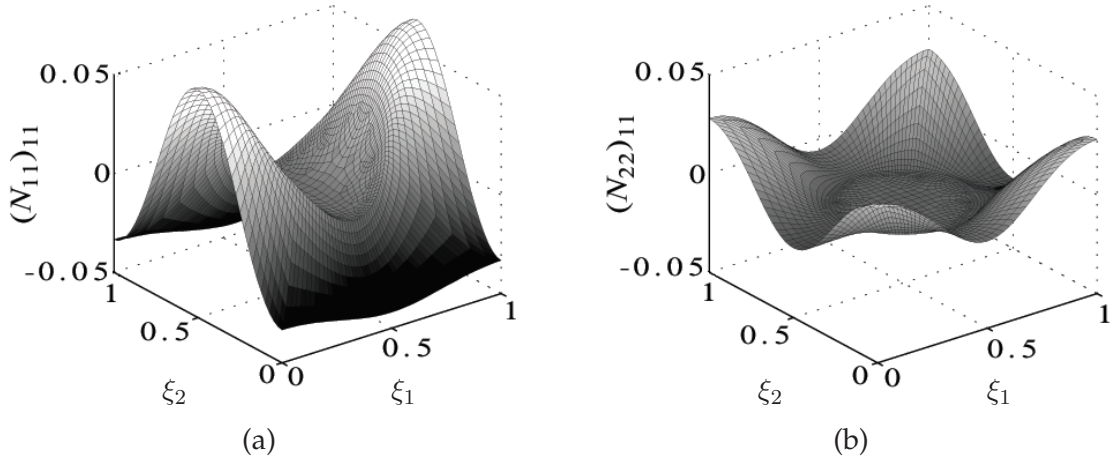

FIGURE 5. Typical components of the second-order problems: **(a)** $(N_{11})_{11}$ and **(b)** $(N_{11})_{22}$

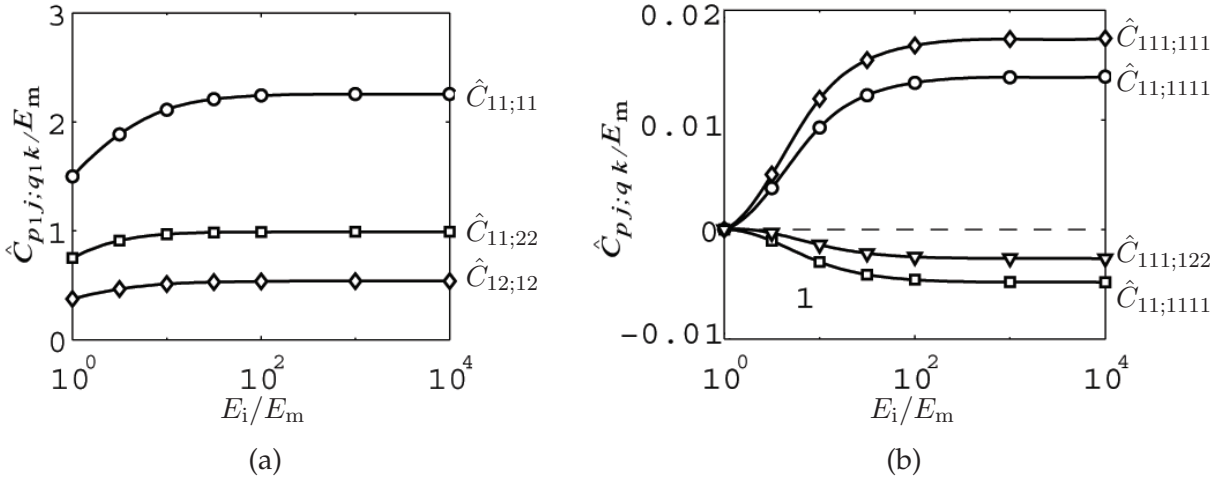

FIGURE 6. Effective moduli of **(a)** standard order ($\hat{C}_{p_1j;q_1k}$) and **(b)** higher order ($\hat{C}_{pj;qk}$) vs. Young's modulus of the fiber; both axes have been normalized by Young's modulus of the matrix

order terms are multiplied by powers of ε in the constitutive law (38). This means that their relevance decreases as the separation between the microstructural and macroscopic scales increases. When this scale separation is relatively small, however, or when strong gradients are present in the averaged displacements $\hat{\mathbf{v}}$, the influence of the higher-order terms will be more noticeable.

In order to examine the influence of the stiffness contrast between inclusion and matrix on the effective properties of the composite, the ratio $E_{\mathrm{i}}/E_{\mathrm{m}}$ has been varied in the range of $1 - 10^4$. The resulting effective moduli, normalized by Young's modulus of the matrix and unit length, have been plotted versus the contrast in Fig. 6. Figure 6(a) shows the moduli $\hat{C}_{ijkl}$ of the standard order. For increasing stiffness of the fiber, the moduli increase from the homogeneous values at $E_{\mathrm{i}} = E_{\mathrm{m}}$ to horizontal asymptotes in the limit of a rigid fiber. Some of the higher-order moduli have been plotted

TABLE 1. Normalized effective higher-order moduli $\hat{C}_{pj;qk}$ computed with the higher-order homogenization method; components not given follow from symmetry or vanish.

$\hat{C}_{11;11}$	=	2.242661	$\hat{C}_{111;111}$	=	0.016795	$\hat{C}_{1111;1111}$	=	0.005738
$\hat{C}_{11;22}$	=	0.990341	$\hat{C}_{111;122}$	=	−0.002489	$\hat{C}_{1111;1122}$	=	−0.002944
$\hat{C}_{12;12}$	=	0.535859	$\hat{C}_{111;221}$	=	0.000973	$\hat{C}_{1111;1221}$	=	−0.001017
$\hat{C}_{11;1111}$	=	0.013393	$\hat{C}_{112;112}$	=	0.007393	$\hat{C}_{1111;2222}$	=	−0.000537
$\hat{C}_{11;1122}$	=	−0.004581	$\hat{C}_{112;121}$	=	0.003496	$\hat{C}_{1112;1112}$	=	0.003235
$\hat{C}_{11;1221}$	=	0.000619	$\hat{C}_{121;121}$	=	0.002746	$\hat{C}_{1112;1121}$	=	0.001559
$\hat{C}_{11;2222}$	=	−0.003646				$\hat{C}_{1112;1222}$	=	0.001130
$\hat{C}_{12;1112}$	=	0.001189				$\hat{C}_{1112;2221}$	=	0.002037
$\hat{C}_{12;1121}$	=	0.000371				$\hat{C}_{1121;1121}$	=	0.001374
						$\hat{C}_{1121;1222}$	=	0.000574
						$\hat{C}_{1122;1122}$	=	0.006014
						$\hat{C}_{1122;1221}$	=	0.004645

in Fig. 6(b); other components show a very similar trend and have been left out for clarity. As should be expected, all higher-order moduli vanish for the homogeneous material ($E_\mathrm{i} = E_\mathrm{m}$). As the degree of heterogeneity increases, however, these higher-order terms become more important. It is interesting to note that they also asymptote to a finite value for a rigid fiber.

5. DISCUSSION AND CONCLUDING REMARKS

The effective properties listed in Table 1 give an impression of the amount of data that can be generated with the numerical homogenization strategy described in this paper. Only two orders of strain gradients have been taken into account, and the number of different moduli is further reduced by the high degree of symmetry of the periodic cell. But already in this case determining a parameter set of this size experimentally would be extremely difficult. Instead, the entire set has been determined solely on the basis of the (four) elastic constants of the constituents and their geometric arrangement. No *a priori* assumptions have been made about the macroscopic behavior of the material. The only assumptions are in the modeling of the microstructure; length-scale effects, anisotropy, and other macroscopic properties all enter the effective representation naturally in the periodic homogenization process. The degree to which these effects are captured is set by the number of higher-order terms that are included (i.e., the parameter K).

Two essential requirements for the method in its present form to work are periodicity of the microstructure and linear elastic material behavior of its constituents. This latter condition has been somewhat alleviated by the extension of the theory to a limited class of nonlinear elasticity problems by Cherednichenko and Smyshlyaev [48]. As to the periodicity assumption, it is emphasized that, although a periodic body force has been assumed in deriving the effective constitutive model, its application is by no means limited to macroscopically periodic problems. The effective moduli are properties of the material and can therefore

also be used for nonperiodic problems. Application to finite-sized bodies, however, requires a more detailed understanding of the higher-order boundary conditions that must be applied in such cases. At free boundaries, it seems natural to set the higher-order tractions that appear at the boundary (see, e.g., [11,22,46]) equal to zero. But in more complicated situations, these boundary conditions should ideally be linked back to the microstructure. A first attempt in this direction — albeit for a nonlocal theory of the integral type — has been undertaken by Luciano [49], but more work is needed to further clarify this link.

Periodicity of the microstructure is an essential condition, which often will not be met for real materials. However, this limitation is less restrictive than it may appear. Microstructures that are not periodic may be dealt with by defining a representative volume element, i.e., a sample volume which is sufficiently large and contains a sufficient number of microstructural features for its periodic extension to be representative of the real, disordered microstructure. Such representative volumes will generally be much larger compared with the microstructural components (e.g., inclusions) than the unit cell of Section 4, but since the homogenization method is based on a body force generating strain gradients within the cell, this does not need to pose a problem. Computationally, however, the microstructural analyses will become more expensive as the number of finite elements needed to describe the microstructure increases.

A drawback of the strain gradient theory that results from the homogenization process is that it imposes stringent continuity requirements on the effective displacement field. This may not be a problem when macroscopic problems can be solved analytically, but it poses a difficulty for numerical analysis methods, such as the finite element method. Particularly for high degrees of microstructural detail (large K), this may seriously complicate the implementation of the macroscopic strain gradient formulation in analysis codes. Replacement of the rigorously derived effective relations by approximate relations, which are easier to deal with in this respect, may be one option here. Or alternatively, and perhaps more attractively, one could aim to adapt the rigorous homogenization framework such that it delivers an effective constitutive description that is more favorable with respect to numerical implementation. These and other aspects of the method, e.g., extensions to the nonlinear regime, provide many opportunities for fruitful further developments.

ACKNOWLEDGMENT

Financial support from the EU-TMR program "Spatial-temporal Instabilities in Deformation and Fracture" (Contract No. FMRX-CT96-0062) is gratefully acknowledged. The authors also wish to thank V.P. Smyshlyaev (University of Bath, UK) and J.R. Willis (University of Cambridge, UK) for helpful discussions.

REFERENCES

1. V. P. Smyshlyaev and K. D. Cherednichenko, On rigorous derivation of strain gradient effects in the overall behaviour of periodic heterogeneous media, *J. Mech. Phys. Solids* **48**:1325–1358, 2000.
2. G. A. Maugin, Nonlinear Waves in Elastic Crystals, Oxford University Press, Oxford, 1999.
3. L. V. Raulea, A. M. Goijaerts, L. E. Govaert, and F. P. T. Baaijens, Size effects in the processing of thin metal sheets, *J. Mater. Process. Technol.* **115**:44–48, 2001.
4. N. A. Fleck, G. M. Muller, M. F. Ashby, and J. W. Hutchinson, Strain gradient plasticity: theory and experiment, *Acta Metall. Mater.* **42**:475–487, 1994.

5. J. S. Stölken and A. G. Evans, A microbend test method for measuring the plasticity length scale, *Acta Mater.* **46**:5109–5115, 1998.
6. C. Chen and N. A. Fleck, Size effects in the constrained deformation of metallic foams, *J. Mech. Phys. Solids* **50**:955–977, 2002.
7. H. H. M. Cleveringa, E. van der Giessen, and A. Needleman, Comparison of discrete dislocation and continuum plasticity predictions for a composite material, *Acta Mater.* **45**:3163–3179, 1997.
8. R. J. M. Smit, W. A. M. Brekelmans, and H. E. H. Meijer, Prediction of the mechanical behaviour of nonlinear heterogeneous systems by multi-level finite element modeling, *Comput. Methods Appl. Mech. Eng.* **155**:181–192, 1998.
9. V. Kouznetsova, M. G. D. Geers, and W. A. M. Brekelmans, Multi-scale constitutive modelling of heterogeneous materials with a gradient-enhanced computational homogenization scheme, *Int. J. Numer. Methods Eng.* **54**:1235–1260, 2002.
10. V. Kouznetsova, M. G. D. Geers and W. A. M. Brekelmans, On the size of a representative volume element in a second-order computational homogenization framework, *Int. J. Multiscale Comput. Eng.* 2:575-598, 2004.
11. R. A. Toupin, Elastic materials with couple-stresses, *Arch. Ration. Mech. Anal.* **11**:385–414, 1962.
12. R. D. Mindlin, Micro-structure in linear elasticity, *Arch. Ration. Mech. Anal.* **16**:51–78, 1964.
13. E. Kröner, Elasticity theory of materials with long range cohesive forces, *Int. J. Solids Struct.* **3**:731–742, 1967.
14. D. G. B. Edelen and N. Laws, On the thermodynamics of systems with nonlocality, *Arch. Ration. Mech. Anal.* **43**:24–35, 1971.
15. A. C. Eringen and D. G. B. Edelen, On nonlocal elasticity, *Int. J. Eng. Sci.* **10**:233–248, 1972.
16. E. Cosserat and F. Cosserat, Théorie des Corps Déformables, Hermann & Fils, Paris, 1909.
17. E. C. Aifantis, On the microstructural origin of certain inelastic models, *J. Eng. Mater. Technol.* **106**:326–330, 1984.
18. Z. P. Bažant, T. Belytschko, and T. P. Chang, Continuum theory for strain-softening, *J. Eng. Mech.* **110**:1666–1692, 1984.
19. B. D. Coleman and M. L. Hodgdon, On shear bands in ductile materials, *Arch. Ration. Mech. Anal.* **90**:219–247, 1985.
20. H.-B. Mühlhaus and E. C. Aifantis, A variational principle for gradient plasticity, *Int. J. Solids Struct.* **28**:845–857, 1991.
21. N. A. Fleck and J. W. Hutchinson, A phenomenological theory for strain gradient effects in plasticity, *J. Mech. Phys. Solids* **41**:1825–1857, 1993.
22. N. A. Fleck and J. W. Hutchinson, Strain Gradient Plasticity, *Advances Appl. Mech.* **33**:295–361, 1997.
23. A. Acharya and J. L. Bassani, Incompatibility and crystal plasticity, *J. Mech. Phys. Solids* **48**:1565–1595, 2000.
24. N. A. Fleck and J. W. Hutchinson, SA reformulation of strain gradient plasticity, *J. Mech. Phys. Solids* **49**:2245–2271, 2001.
25. G. Pijaudier-Cabot and Z. P. Bažant, Nonlocal damage theory, *J. Eng. Mech.* **113**:1512–1533, 1987.
26. R. de Borst and H.-B. Mühlhaus, Gradient-dependent plasticity: formulation and algorithmic aspects, *Int. J. Numer. Methods Eng.* **35**:521–539, 1992.
27. R. H. J. Peerlings, R. de Borst, W. A. M. Brekelmans, and J. H. P. de Vree, Gradient-enhanced damage for quasi-brittle materials, *Int. J. Numer. Methods Eng.* **39**:3391–3403, 1996.
28. J. Y. Shu, W. E. King, and N. A. Fleck, Finite elements for materials with strain gradient effects, *Int. J. Numer. Methods Eng.* **44**:373–391, 1999.
29. M. G. D. Geers, R. L. J. M. Ubachs, and R. A. B. Engelen, Strongly nonlocal gradient-enhanced finite strain elastoplasticity, *Int. J. Numer. Methods Eng.* **56**:2039–2068, 2003.
30. Z. P. Bažant, G. Pijaudier-Cabot, and R. A. B. Engelen, Measurement of characteristic length of nonlocal continuum, *J. Eng. Mech.* **115**:755–767, 1989.
31. M. G. D. Geers, R. de Borst, W. A. M. Brekelmans, and R. H. J. Peerlings, Validation and internal length scale determination for a gradient

damage model: application to short glass-fibre-reinforced polypropylene, *Int. J. Solids Struct.* **36**:2557–2583, 1999.

32. R. Hill, Elastic properties of reinforced solids: Some theoretical principles, *J. Mech. Phys. Solids* **11**:357–372, 1963.
33. T. Mori and K. Tanaka, Average stress in matrix and average elastic energy of materials with misfitting inclusions, *Acta Metall.* **21**:571–574, 1973.
34. A. Bensoussan, J.-L. Lions, and G. C. Papanicolaou, *Asymptotic Analysis for Periodic Structures*, North Holland, Amsterdam, 1978.
35. E. Sanchez-Palencia, *Nonhomogeneous Media and Vibration Theory*, vol. 27 Lecture Notes in Physics. Springer, Berlin, 1980.
36. J. R. Willis, The overall elastic response of composite materials, *J. Appl. Mech.* **50**:1202–1209, 1983.
37. S. Nemat-Nasser and M. Hori, *Micromechanics: Overall Properties of Heterogeneous Materials*, Elsevier, Amsterdam, 1993.
38. W. J. Drugan and J. R. Willis, A micromechanics-based nonlocal constitutive equation and estimates of representative volume element size for elastic composites, *J. Mech. Phys. Solids* **44**:497–524, 1996.
39. R. Luciano and J. R. Willis, Non-local constitutive response of a random laminate subjected to configuration-dependent body force, *J. Mech. Phys. Solids* **49**:431–444, 2001.
40. M. J. Beran and J. J. McCoy, Mean field variations in a statistical sample of heterogeneous linearly elastic solids, *Int. J. Solids Struct.* **6**:1035–1054, 1970.
41. M. J. Beran and J. J. McCoy, The use of strain gradient theory for analysis of random media, *Int. J. Solids Struct.* **6**:1267–1275, 1970.
42. C. Boutin, Microstructural effects in elastic composites, *Int. J. Solids Struct.* **33**:1023–1051, 1996.
43. N. Triantafyllidis and S. Bardenhagen, The influence of scale size on the stability of periodic solids and the role of associated higher order gradient continuum models, *J. Mech. Phys. Solids* **44**:891–1928, 1996.
44. R. H. J. Peerlings and N. A. Fleck, Numerical analysis of strain gradient effects in periodic media, *J. de Phys. IV* **11**:153–160, 2001.
45. N. Bakhvalov and G. Panasenko, *Homogenisation: Averaging Processes in Periodic Media*, Kluwer, Dordrecht, 1989.
46. R. D. Mindlin, Second gradient of strain and surface-tension in linear elasticity, *Int. J. Solids Struct.* **1**:417–438, 1965.
47. R. H. J. Peerlings and N. A. Fleck, Enriched effective modelling of elastic periodic composites, *Proc. of 2nd European Conference on Computational Mechanics*, Cracow, Poland. (CD-ROM), Z. Waszczyszyn and J. Pamin (eds.), Cracow University of Technology, 2001.
48. K. D. Cherednichenko and V. P. Smyshlyaev, On full asymptotic expansion of the solutions of nonlinear periodic rapidly oscillating problems, Preprint NI99028-SMM, Isaac Newton Institute for Mathematical Sciences, Cambridge, UK, 1999.
49. R. Luciano and J. R. Willis, Boundary-layer corrections for stress and strain fields in randomly heterogeneous materials, *J. Mech. Phys. Solids* **51**:1075–108, 2003.